STEM CELLS®

TRANSLATIONAL AND CLINICAL RESEARCH

Protective Effects of Human iPS-Derived Retinal Pigmented Epithelial Cells in Comparison with Human Mesenchymal Stromal Cells and Human Neural Stem Cells on the Degenerating Retina in *rd1* Mice

JIANAN SUN,[a,b] MICHIKO MANDAI,[a] HIROYUKI KAMAO,[a,c] TOMOYO HASHIGUCHI,[a] MASAYUKI SHIKAMURA,[d] SHIN KAWAMATA,[d] SUNAO SUGITA,[a] MASAYO TAKAHASHI[a]

Key Words. Transplantation • Cell-based therapy • Induced pluripotent stem cells • Retinal pigment epithelium cells • Retinal degeneration • Pigment epithelium-derived factor

[a]Laboratory for Retinal Regeneration, RIKEN Center for Developmental Biology (CDB), Kobe, Japan; [b]Application Biology and Regenerative Medicine, Graduate School of Medicine, Kyoto University, Kyoto, Japan; [c]Department of Ophthalmology, Kawasaki Medical School, Kurashiki, Okayama, Japan; [d]Research and Development Center for Cell Therapy, Foundation for Biomedical Research and Innovation, Kobe, Japan

Correspondence: Michiko Mandai, Ph.D., M.D., Laboratory for Retinal Regeneration, RIKEN Center for Developmental Biology, 2-2-3 Minatojima Minamimachi, Chuo-ku, Kobe, Hyogo 650-0047, Japan. Telephone: 81-78-306–3305; Fax: 81-78-306–3303; e-mail: mmandai@cdb.riken.jp

Received September 15, 2014; accepted for publication December 26, 2014; first published online in STEM CELLS *EXPRESS* February 28, 2015.

1066-5099/2014/$30.00/0

http://dx.doi.org/10.1002/stem.1960

ABSTRACT

Retinitis pigmentosa (RP) is a group of visual impairments characterized by progressive rod photoreceptor cell loss due to a genetic background. Pigment epithelium-derived factor (PEDF) predominantly secreted by the retinal pigmented epithelium (RPE) has been reported to protect photoreceptors in retinal degeneration models, including *rd1*. In addition, clinical trials are currently underway outside Japan using human mesenchymal stromal cells and human neural stem cells to protect photoreceptors in RP and dry age-related macular degeneration, respectively. Thus, this study aimed to investigate the rescue effects of induced pluripotent stem (iPS)-RPE cells in comparison with those types of cells used in clinical trials on photoreceptor degeneration in *rd1* mice. Cells were injected into the subretinal space of immune-suppressed 2-week-old *rd1* mice. The results demonstrated that human iPS-RPE cells significantly attenuated photoreceptor degeneration on postoperative days (PODs) 14 and 21 and survived longer up to at least 12 weeks after operation than the other two types of graft cells with less immune responses and apoptosis. The mean PEDF concentration in the intraocular fluid in RPE-transplanted eyes was more than 1 μg/ml at PODs 14 and 21, and this may have contributed to the protective effect of RPE transplantation. Our findings suggest that iPS-RPE cells serve as a competent source to delay photoreceptor degeneration through stable survival in degenerating ocular environment and by releasing neuroprotective factors such as PEDF. STEM CELLS *2015;33:1543–1553*

INTRODUCTION

Retinitis pigmentosa (RP), characterized by inherited, progressive cell loss leading to atrophy of the retinal tissue in advanced cases, is one of the most severe retinal degeneration diseases. The prevalence of RP is approximately 1:5,000 worldwide. Although no definite effective intervention has been reported till date, a number of therapeutic strategies have been explored to treat RP patients. Among these, cell therapy has been considered to be a promising approach.

Retinal pigmented epithelium (RPE) cells form a monolayer sheet between the neurosensory retina and the choroid and perform several essential functions in the eye, such as phagocytosis of photoreceptor outer segments, maintenance of the visual cycle, secretion of trophic factors, and immune modulation [1]. In 1988, RPE cells were successfully transplanted into the subretinal space of Royal College of Surgeons (RCS) rats (*Mertk* −/−), a classic animal model for retinal degeneration [2], and RPE transplantation has received considerable attention since then. It was considered beneficial to replace dysfunctional RPE cells in age-related macular degeneration (AMD) or certain types of RP caused by RPE dysfunctions such as those with *RPE65* or *MERTK* gene mutations [3, 4]. Conversely, pigment epithelium-derived factor (PEDF) is abundantly secreted by RPE cells [5, 6], and numerous studies have shown that it can protect neurons from cell death through induction by various factors, including glutamate [7], hydrogen peroxide [8], light [9], ischemic injury [10], and inherited disease (e.g., photoreceptor degeneration in *rd1* mice) [11]. These data suggest that transplanted RPE not only replaces the dysfunctional cells but also acts as a source of trophic factor secretion.

In addition to RPE cells, Müller cells [12], ocular resident stem cells [13], and adult tissue stem cells (including mesenchymal stromal cells [MSCs] [14–16] and neural stem cells [NSCs] [17–19]) have been used for transplantation in an attempt to protect or substitute for degenerating neurons in retinal or other neuronal degenerative disorders. At present, there are two clinical trials underway using MSCs and NSCs to prevent photoreceptor degeneration in RP (ID: NCT01531348; https://www.clinicaltrials.gov) and AMD (ID: NCT01632527), respectively. Thus, for future clinical applications, it is worthy to investigate the comparative advantages of these cells in preventing the neurodegenerative process caused by photoreceptor loss. In this study, we compared the neuroprotective efficacy of subretinal transplanted-induced pluripotent stem (iPS)-RPE cells, MSCs, and NSCs in a rapid retinal degeneration model of RP, *rd1* mice. This model contains a nonsense mutation in the gene encoding the beta subunit of the rod photoreceptor-specific cGMP phosphodiesterase 6 (PDE 6). This causes severe, early-onset photoreceptor degeneration beginning around postnatal day (P) 10, with a maximum peak around P14 [20, 21].

This preclinical proof-of-concept study demonstrated that compared with MSCs and NSCs, iPS-RPE cells significantly protected photoreceptor cells from degeneration in *rd1* mice up to postoperative day (POD) 21. In addition, they displayed a superior graft survival of no less than 12 weeks, even in the severe degenerative environment of xenografting. Thus, iPS-RPE cells may serve as a potential resource to protect photoreceptors, even under severely degenerating conditions such as those common in RP or AMD.

Materials and Methods

Cell Preparation

Human iPS cells, generously provided by the Center for iPS Cell Research and Application, Kyoto University (Kyoto, Japan), were maintained and differentiated to RPE cells as described previously [22].

Human fetal NSCs (Cat. No. HNS-COR-001) were purchased from SC Proven Product sold by StemCells, Inc (Newark, CA, http://www.stemcellsinc.com), which sponsored the abovementioned AMD clinical trial. Cells were maintained and passaged as per the manufacturer's recommendations. (Nevertheless, these cells were not derived and produced in the same manner as the cells being tested in clinical studies)

A nonclinical experiment was implemented to derive MSCs from donated umbilical cords. Both the experiment and the related informed consent forms were reviewed and approved by the Institutional Review Board of the Riken Center for Developmental Biology (CDB) and the Foundation for Biomedical Research and Innovation. Refer to Supporting Information Experimental Procedures for more details regarding cell culture.

For transplantation, RPE cells and MSCs were harvested with 0.25% Trypsin-EDTA (Life Technologies, Carlsbad, CA, https://www.lifetechnologies.com). NSCs were harvested with Accutase (Sigma-Aldrich, St. Louis, MO, http://www.sigmaaldrich.com) and washed twice with Glasgow Minimum Essential Medium (Life Technologies), which was also used as the delivery medium for all three cell types. To reduce cell clumping, DNase I (Stem Cell Technologies, Vancouver, Canada, http://www.stemcell.com) was added to the cell suspensions (final: 0.1 mg/ml).

Flow Cytometry

The following antibodies: CD73-FITC, CD90-APC, CD105-PE, and CD146-PE (all from BD Biosciences, San Jose, CA, https://www.bdbiosciences.com) were used for identifying MSCs. For details, see Supporting Information Experimental Procedures.

Immunostaining

Primary antibodies against nestin, beta-3 tubulin (Tuj1), MAP2, vimentin, bestrophin, RPE65, MITF, ZO-1, human Ki67, human CD147, human nuclei antigen, human beta-2 microglobulin, Iba1, CD3, and rhodopsin (Supporting Information Table S1) were used to stain samples. For details, see Supporting Information Experimental Procedures.

Transplantation

Surgical procedures were performed on 14-day-old C3H/HeJ mice, which are homozygous for the *rd1* mutation (*Pde6b*$^{rd1-/rd1-}$). All animal experiments were in accordance with the Association for Research in Vision and Ophthalmology statement for the Use of Animals in Ophthalmic and Vision Research and the Guidelines of the Riken CDB Animal Experiment Committee. Drinking water containing 200 mg/l cyclosporine (Wako, Osaka, Japan, http://www.wako-chem.co.jp) and 10 mg/l indomethacin (Wako) was provided to all animals from 2 days prior to transplantation until the time of sacrifice. The mice were sedated with an intramuscular injection of a combination of ketamine (77 mg/kg, Daiichi-Sankyo, Tokyo, Japan, http://www.daiichisankyo.com) and xylazine (10 mg/kg, Bayer, Leverkusen, Germany, http://www.bayer.com), and pupils were dilated with a mixture of tropicamide (5 mg/ml, Santen, Osaka, Japan, http://www.santen.com) and phenylephrine (5 mg/ml, Santen). After making a trans-scleral incision, we delivered 1×10^5 cells (in 1 μl delivery medium) into the subretinal space of one eye of each animal through a syringe (Hamilton, Reno, NV, http://www.hamiltoncompany.com) with a 33-gauge needle. A bleb formed following injection, and the needle was kept in the bleb for a few seconds to prevent efflux of the transplanted cells into the vitreous. Using the same procedure, 1 μl delivery medium was injected into the subretinal space of the contralateral eye as a vehicle control. Immediately following the operation, the fundus was carefully examined for retinal or vascular damage or signs of cell efflux. Mice with such problems were excluded from the experiment. For each experiment, four different batches of mice (five mice/batch) at p14 were transplanted with one cell type and the mice with successful transplantation were used randomly in each cell-type group to the downstream time-dependent analysis. Cell viability was also checked to be more than 90% at the end of transplantation for each cell type.

Enzyme-Linked Immunosorbent Assay

Following 48 hours of incubation, the culture medium was collected from cells just before transplantation and stored at −80°C until analysis. The cultured cells were then dissociated and counted to present data as protein produced per 48 hours per million cells. The final concentrations of cytokines secreted by each cell type were obtained by subtracting the culture

medium values of each cell type. Intraocular fluid (IF) specimens from grafted and sham eyes also were collected at PODs 7, 14, and 21. Enzyme-linked immunosorbent assay (ELISA) kits for brain-derived neurotrophic factor (BDNF), insulin-like growth factor 1 (IGF-1), transforming growth factor beta-2 (TGF-beta-2) (all from R&D Systems, Minneapolis, MN, https://www.rndsystems.com), beta-nerve growth factor (beta-NGF), neurotrophin-3 (NT-3) ciliary neurotrophic factor (CNTF) (all from Raybiotech, Atlanta, GA, http://www.raybiotech.com), glial cell line-derived neurotrophic factor (GDNF) (Promega, Fitchburg, WI, https://www.promega.com), PEDF (Biovendor, Czech Republic, http://www.biovendor.com), and vascular endothelial growth factor (VEGF) (eBioscience, San Diego, CA, http://www.ebioscience.com) were used according to manufacturers' protocols. ELISA plates were analyzed using a microplate photometer (Thermo, Waltham, MA, http://www.thermofisher.com).

Terminal Deoxynucleotidyl Transferase dUTP Nick End Labeling Assay

To detect apoptotic cells, retinal sections were processed for transferase dUTP nick end labeling (TUNEL) using a kit (Roche, Basel, Switzerland, http://www.roche.com) according to the manufacturer's instructions. Sections were double labeled by specific primary antibodies as described elsewhere.

Quantitative Analysis

Every first slide per each sample series (sections of every 50 μm) from PODs 14 and 21 was stained, and the number of rhodopsin-positive rods was counted. The total number was the sum of each series. With regard to graft cell survival, we used two parameters: the number of graft cells on the section series that contained the largest graft number and the length of graft area calculated by the total number of the sections containing the graft (Fig. 3H). In addition, to express proliferation, apoptosis, and immune reaction as the percentage of the number of Ki67-, TUNEL-, and Iba1-positive cells to the total graft cell number of each section, respectively, we chose the slides of the series containing the greatest number of graft cells in each eye sample for TUNEL assay and immunostaining. All these cell countings were performed by a single person in a masked manner as to transplanted cell types, and also transplanted or control eyes.

Statistical Analysis

All data were analyzed with SPSS 19.0 (IBM, Chicago, IL, http://www.spss.com) and expressed as the mean ± SD. Multiple comparisons were performed by one-way ANOVA, followed by post hoc Bonferroni tests unless otherwise stated. Unpaired *t* test was conducted to compare the number of the remaining rods in grafts transplanted eyes and in sham injected fellow eyes. Statistical significance was denoted as *, $p < .05$ and **, $p < .01$.

Results

In Vitro and In Vivo Characterization of iPS-RPE Cells, MSCs, and NSCs

Prior to use, MSCs, NSCs, and iPS-RPE cells were characterized by immunocytochemistry or flow cytometry. In vitro, iPS-RPE cells formed a pigmented monolayer with a typical hexagonal appearance (Fig. 1A) and stained positive for a panel of RPE markers, including MITF, ZO-1, bestrophin, and RPE65 (Fig. 1C, 1D, 1G, 1H).

For NSCs, the immature NSC markers nestin and vimentin (Fig. 1M, 1P) were obviously detected in vitro, while a more mature marker, Tuj1, as well as a mature neuron marker, MAP2, were negative (Fig. 1L, 1Q). Consistent with previous studies, the transplanted NSCs remained undifferentiated, continually expressing nestin and vimentin for the entire duration of the study (Supporting Information Fig. S1).

We evaluated human MSCs for expression of the reported surface markers CD105, CD73, and CD90 [23], and additionally CD146 to distinguish them from human fibroblasts, which were recently reported to be positive for CD73, CD90, and CD105 [24, 25]. In addition, because aging is another concern for MSC transplantation [26], CD146 was used as an indicator of replicative MSC senescence [27]. Moreover, CD73 and CD90 were reported to decline with aging [27]. MSCs used for transplantation were positive for CD105 (100%), CD90 (100%), and CD73 (97.5%) and showed high expression of CD146 (nearly 70%) (Fig. 1T–1W). As such, we reasonably estimated that these cells were adequate for our experimental purpose.

Prior to transplantation, these three cell types were also tested for their potency in secreting trophic factors. Thus, before harvesting cells for transplantation, we collected the medium for testing a number of trophic factors previously reported to be produced by one or more of these cell types [28–36]. ELISA data confirmed that iPS-RPE cells prominently secreted PEDF (240,227 ± 61,878 pg/ml/10^6/48 hours) as compared to 8,304 ± 947 and 181 ± 34 pg/ml/10^6/48 hours by MSCs and NSCs, respectively ($p < .01$). Furthermore, iPS-RPE cells released large amounts of VEGF (2,952 ± 358 pg/ml/10^6/48 hours) and TGF-beta-2 (198 ± 1 pg/ml/10^6/48 hours) and small amounts of beta-NGF (4 ± 1 pg/ml/10^6/48 hours) and NT-3 (8 ± 1 pg/ml/10^6/48 hours). A lower concentration of TGF-beta-2 (82 ± 52 pg/ml/10^6/48 hours) was also detected in the NSC supernatant. MSCs produced BDNF (20 ± 2 pg/ml/10^6/48 hours), which was found in neither the iPS-RPE cell nor the NSC supernatant. Neurotrophic factors IGF-1, CNTF, and GDNF were not detected in the conditioned medium of any cell type (Fig. 1X; $n = 3$ for each type of cells).

Assessment of the Protective Effects of the Grafts on Degenerating Photoreceptors and Graft Viability

To compare the protective effects of the different graft cell types, we quantified the total number of rhodopsin-positive rod photoreceptor cells per eye at PODs 14 and 21. Compared with MSCs and NSCs transplanted group, iPS-RPE cells showed a substantial protective effect on the loss of rod cells (Fig. 2A; $p < .01$, $n = 5$–6. Fig. 2B; RPE vs. MSC, $p < .05$, and RPE vs. NSC, $p < .01$, $n = 5$–7). The outer nuclear layer over the transplantation area of grafted iPS-RPE cells contains more rhodopsin-positive photoreceptors than that of grafted NSCs, MSCs (Fig. 2C–2E), and nongrafted eyes. In the area away from the transplanted region in the iPS-RPE cell-transplanted eyes, rods were minimally observed (Fig. 2F). However, in some cases, the position-associated protective effect was not apparent, but to some extent the remaining rods were dispersed. Moreover, MSCs and NSCs transplanted eyes did not show any statistical significance comparing with their corresponding contralateral sham operated eyes at PODs 14 and 21. The number

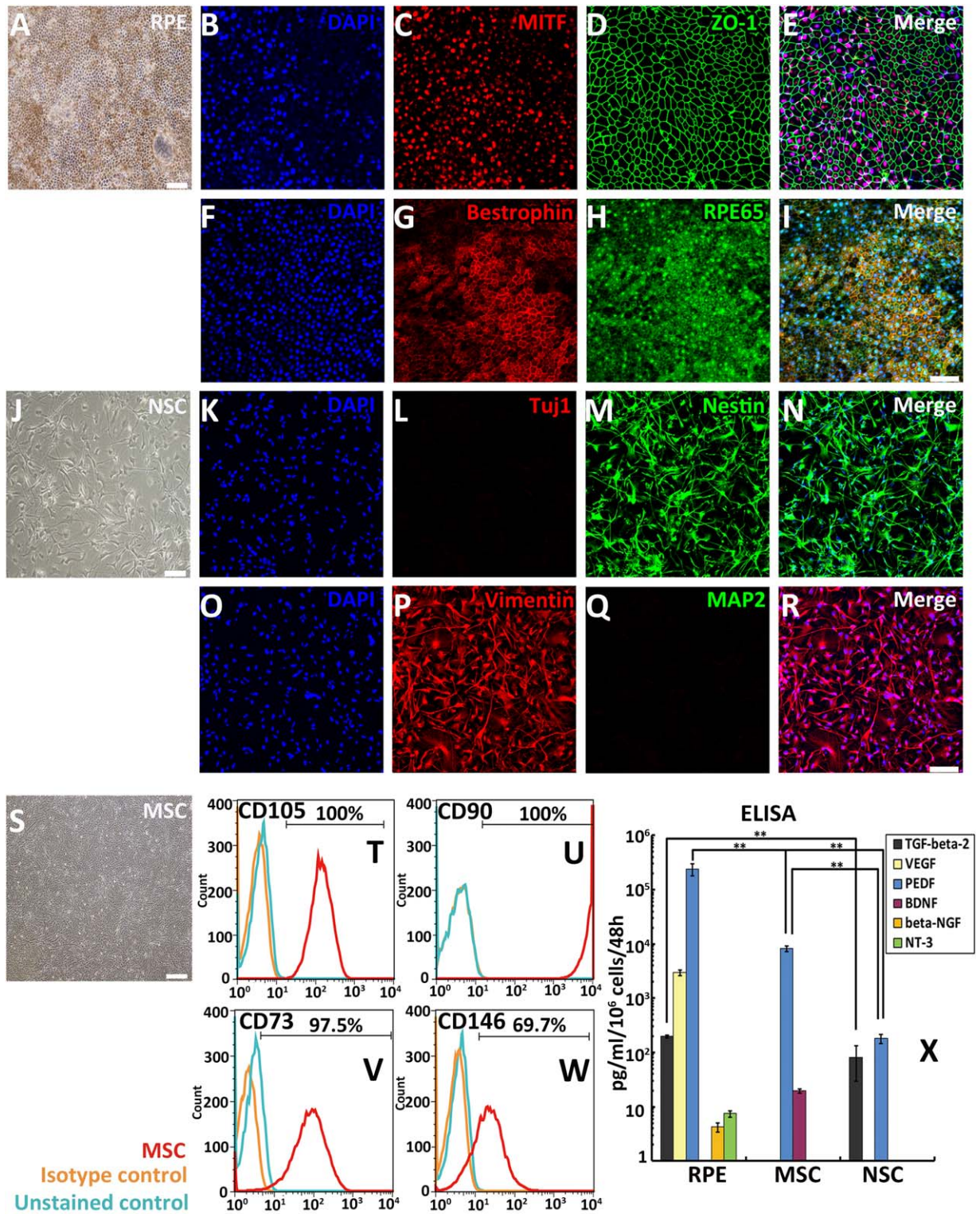

Figure 1. Characterization of human induced pluripotent stem (iPS)-RPE cells, NSCs, and MSCs and the concentration of trophic factors secreted by each cell type before transplantation. **(A, J, S):** Bright-field images of iPS-RPE cells (A), NSCs (J), and MSCs (S). Scale bar in (A) and (J) = 100 μm; scale bar in (S) = 500 μm. Representative immunocytochemical analysis of iPS-RPE cells **(B–I)** and human NSCs **(K–R)**. iPS-RPE cells express typical RPE markers, MITF (C), ZO-1 (D), bestrophin (G), and RPE65 (H). Immature NSC markers, nestin (M) and vimentin (P), were both positive, while mature markers, Tuj1 (L) and MAP2 (Q), were negative. Cell nuclei were detected with DAPI (B, F, K, O), and merged images are shown in panels (E, I, N, R). Scale bar in (I) = 50 μm (also applies to B–H); scale bar in (R) = 100 μm (also applies to K–Q). **(T, U, V, W):** Flow cytometric histogram plots show high expression of putative and essential MSC markers, CD105 (T), CD90 (U), CD73 (V), and CD146 (W). (X): High amounts of several neurotrophic factors were detected in the supernatant of iPS-RPE cells in comparison with that of NSCs and MSCs (**, $p < .01$). Abbreviations: MSC, mesenchymal stromal cell; NSC, neural stem cell; RPE, retinal pigmented epithelium.

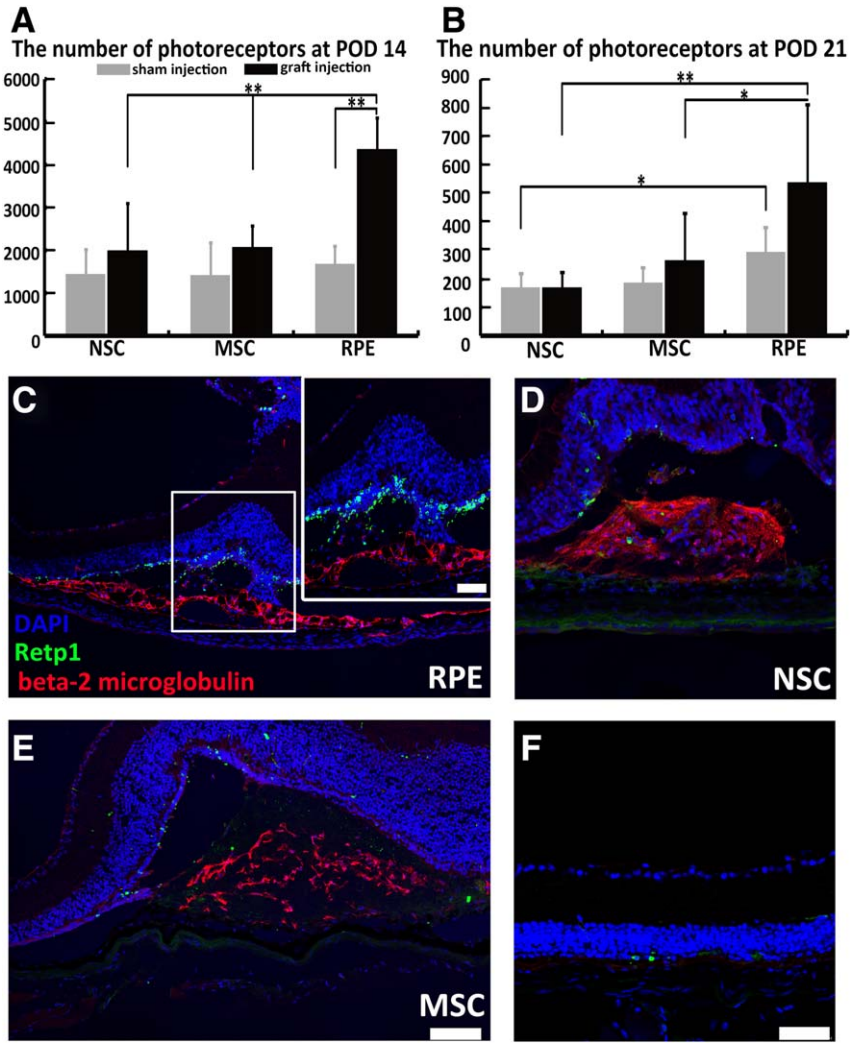

Figure 2. Significant photoreceptor preservation was achieved by PODs 14 and 21 in induced pluripotent stem (iPS)-RPE cells transplanted eyes. **(A, B):** A statistically significant number of rhodopsin-positive photoreceptors was quantified in iPS-RPE grafted eyes in comparison with NSC and MSC grafted and unoperated eyes at PODs 14 (A) and 21 (B). Additionally, the number of remaining rod cells in the sham operated contralateral eyes of the iPS-RPE cells transplanted mice was significantly larger than that of the NSCs transplanted mice at POD 21 (B) (*, $p < .05$; **, $p < .01$; unpaired *t* test was used to compare the number of rod photoreceptors in grafted eyes and sham injected contralateral eyes). **(C–F):** Cross-sections were obtained from eyes at POD 14. Each human cell type was labeled by human beta-2 microglobulin. A representative image of an eye with iPS-RPE injection (C) shows significant extensive rescue of photoreceptors; however, NSC (D) and MSC (E) groups failed. Rod photoreceptor cells were hardly observed in the area far from the site of transplantation in the same iPS-RPE cell-transplanted eye (F). Inset in panel (C) shows a higher magnification of the boxed area. Scale bar in (E) = 100 μm (also applies to C); scale bar in (F) = 50 μm (also applies to D); scale bar in inset = 50 μm. Abbreviations: MSC, mesenchymal stromal cell; NSC, neural stem cell; POD, postoperative day; RPE, retinal pigmented epithelium.

of the remaining rod cells in the sham operated contralateral eyes of the iPS-RPE cells transplanted mice was significantly larger than that of the NSCs transplanted mice at POD 21 (Fig. 2B; $p < .05$). iPS-RPE-injected eyes did not show a remarkable number of photoreceptor cells remaining at the 8th and 12th weeks, suggesting that the effect was a delay in photoreceptor loss upon iPS-RPE transplantation (data not shown).

We then evaluated the duration of the graft survival in these three cell types. Considering the cell-based effect, we evaluated the number of surviving cells by two parameters: the length of graft area (Fig. 3A) and the number of cells in the section with the largest cell number in each eye (Fig. 3B). Following transplantation, iPS-RPE graft cells spread over a larger area than the other cell types at any time point (Fig. 3A; POD 1, RPE vs. MSC and NSC, $p < .05$; PODs 3, 7, 14, and 21, RPE vs. MSC and NSC, $p < .01$; PODs 1, 3, and 7, $n = 3$–4, PODs 14 and 21, $n = 5$–7). In addition, although the length of iPS-RPE grafts decreased over time (Fig. 3C; POD 21 vs. PODs 56 and 84, $p < .01$; POD 21, $n = 6$, POD 56, $n = 3$, POD 84, $n = 3$), iPS-RPE cells were still present at the 8th and 12th week with a transplantation area length of approximately 547 ± 55 μm and 350 ± 132 μm, respectively. The latter was almost equal to that of NSCs (421 ± 160 μm) and MSCs (275 ± 69 μm) at POD 21 (Fig. 3A). Transplanted iPS-RPE cells tended to spread in a tangential direction rather than forming clumps, with some grafts featuring a sheet-like

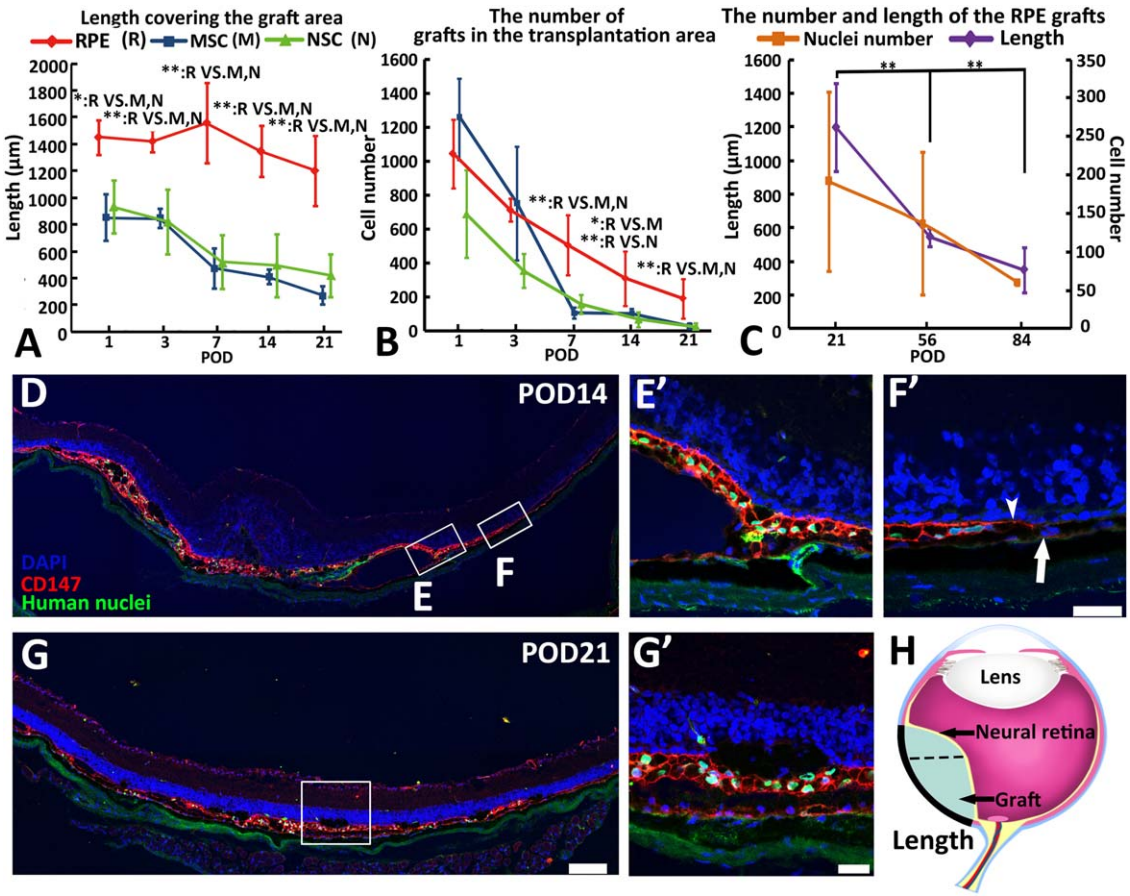

Figure 3. Evaluation of graft survival following human induced pluripotent stem (iPS)-RPE, MSC, and NSC transplantation. **(A, B):** iPS-RPE cell-engrafted eyes displayed a significantly longer transplantation area at multiple time points (A) and contained more grafts from POD 7 in comparison with the other two cell types (B). (A) and (B) share the same graph key (*, $p < .05$; **, $p < .01$). **(C):** The length of the transplantation area at POD 21 showed a significant difference compared with that at PODs 56 and 84 (**, $p < .01$). The graft number was 137 ± 93 and 61 ± 3 at PODs 56 and 84, respectively. **(D, G):** iPS-RPE cells spread in the subretinal space at PODs 14 (D) and 21 (G) and formed a partial sheet-like layer. Human iPS-RPE cells were costained with human CD147 and a human nuclear marker. **(E′, F′):** High-power view of boxes (E) and (F) in panel (D), respectively. Note the observation of an obvious border (arrow head in F′) between human iPS-RPE and the host RPE layer (arrow in F′). **(G′):** High magnification of the boxed area in panel (G). Scale bar in (G) = 100 μm (also applies to D); scale bar in (F′) and (G′) = 20 μm (also applies to E′). **(H):** Cartoon schematic depicts the transplantation area of the eye. "Length" (black bold line) is the distance covering the grafts, and sections (dashed line in H) with the largest number of grafts were selected for cell count and other analyses. Abbreviations: MSC, mesenchymal stromal cell; NSC, neural stem cell; POD, postoperative day; RPE, retinal pigmented epithelium.

structure (Fig. 3D, 3G; Supporting Information Fig. S2A, S2B). The section series with the highest number of grafts in each sample were selected to manually count the grafted human cells. Although there was no statistical significance among the three groups at PODs 1 and 3, iPS-RPE grafts showed a higher cell number than MSC and NSC grafts at all time points thereafter (Fig. 3B; PODs 7 and 21, RPE vs. MSC and NSC, $p < .01$; POD 14, RPE vs. MSC, $p < .05$ and RPE vs. NSC, $p < .01$; PODs 1, 3, and 7, $n = 3$–4, PODs 14 and 21, $n = 5$–7).

Graft Proliferation, Apoptosis, and Immune Reactions in or Around the Graft Site

To better understand the possible reasons for the improved survival of iPS-RPE cells, we next tested proliferation, apoptosis, and immune rejection of each cell type at PODs 1, 3, 7, 14, and 21.

To this end, we used a proliferation marker (Ki67) for investigating the in vivo proliferation of grafts. NSCs showed a robust proliferation compared with the other two cell types at POD 1 (Fig. 4A; $p < .01$; POD 1, $n = 3$). Nevertheless, the proliferation rate dramatically decreased after POD 1, whereas iPS-RPE cells showed an elevated proliferation at POD 3, following which it gradually decreased. In addition, there was no obvious change in MSC proliferation until POD 21. Taken together, the proliferation rates of iPS-RPE cells were significantly higher from POD 3 to 21 than those of MSCs or NSCs (Fig. 4A; POD 3, RPE vs. MSC, $p < .05$ and RPE vs. NSC, $p < .01$; POD 7, RPE vs. MSC and NSC, $p < .01$; PODs 14 and 21, RPE vs. NSC, $p < .01$; PODs 3 and 7, $n = 3$–4, PODs 14 and 21, $n = 5$–7; Supporting Information Fig. S3).

To evaluate the cells' immune reaction, we studied the time-dependent change in the ratio of the number of Iba1-positive microglias in and surrounding the grafts to the total number of grafts (Fig. 4B). With the exception of PODs 1 and 3, eyes receiving the MSC injection showed increased accumulation of microglia than those receiving the NSC and/or iPS-RPE injection (Fig. 4B; POD 7, MSC vs. NSC, $p < .05$, and MSC vs. RPE, $p < .01$; POD 14, MSC vs. RPE, $p < .05$; POD 21,

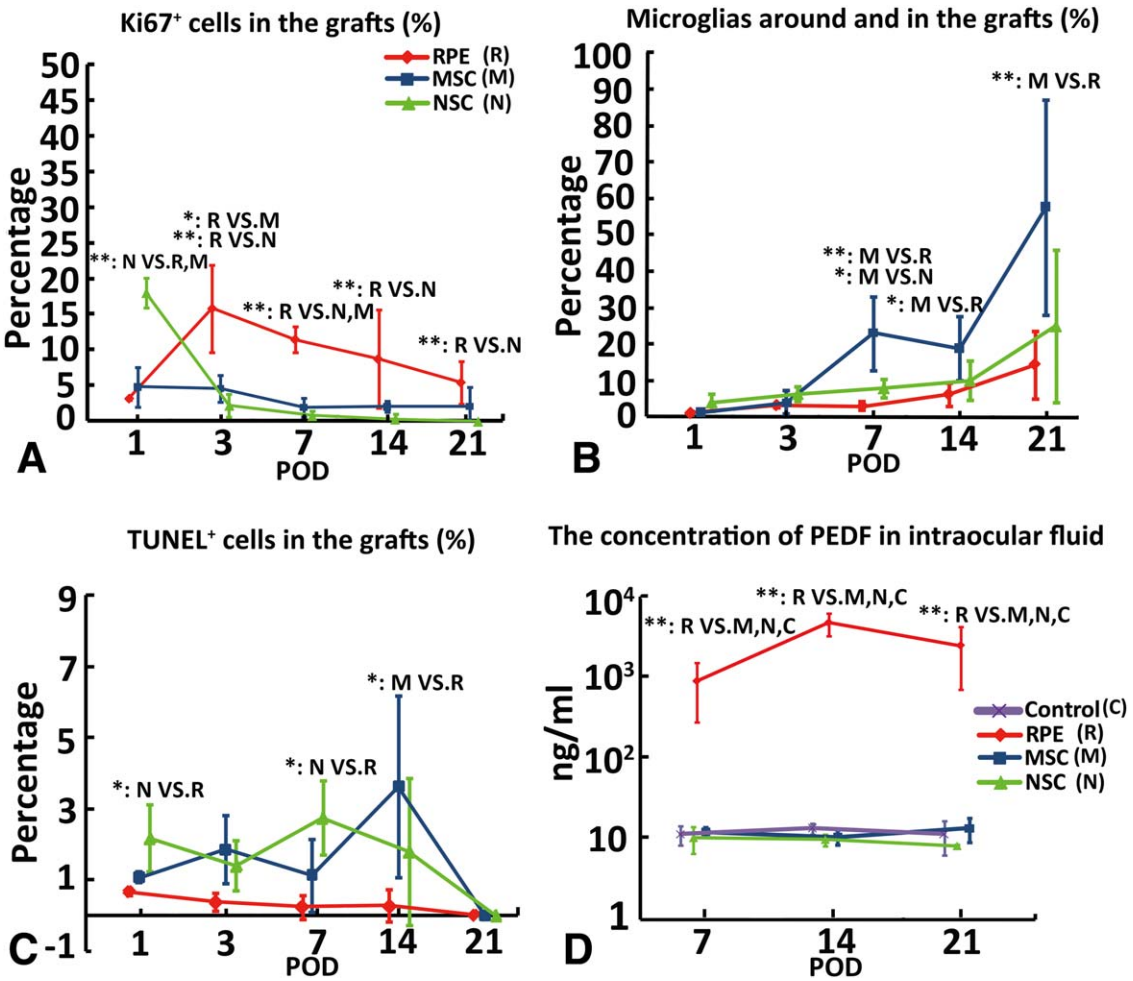

Figure 4. Transplanted induced pluripotent stem (iPS)-RPE cells displayed a higher proliferation rate, lower apoptosis, and mild immune reaction and released a significantly pronounced amount of PEDF in vivo. **(A–C):** Proliferation, immune reaction, and apoptosis were expressed as the percentage of the number of Ki67-, Iba1-, and TUNEL-positive cells to the total number of graft cells of each section, respectively. Except for POD 1, iPS-RPE cells had a higher proliferation rate than NSCs and/or MSCs (A) (Kruskal-Wallis nonparametric test was applied to PODs 14 and 21). Obvious microglial infiltration was observed in the transplantation area of MSC grafted eyes at certain time points (B). NSCs at PODs 1 and 7 and MSCs at POD 14 presented a higher percentage of TUNEL-positive cells, while iPS-RPE cells maintained a low apoptosis rate (C). (A), (B), and (C) share the same graph key (*, $p < .05$; **, $p < .01$). **(D):** Enzyme-linked immunosorbent assay results indicate that the amount of PEDF detected in iPS-RPE-transplanted eyes was statistically significant compared with that detected in NSCs and MSCs transplanted eyes, and sham injected eyes (control) of human iPS-RPE-transplanted mice (**, $p < .01$). Abbreviations: MSC, mesenchymal stromal cell; NSC, neural stem cell; PEDF, pigment epithelium-derived factor; POD, postoperative day; RPE, retinal pigmented epithelium.

MSC vs. RPE, $p < .01$; PODs 1, 3, and 7, $n = 3$–4, PODs 14 and 21, $n = 5$–7; Supporting Information Fig. S4). This may be attributed to the fact that iPS-RPE cells and NSCs release TGF-beta-2, a cytokine that functions to regulate the activation and proliferation status of microglia [37, 38]. Interestingly, we observed no significant infiltration of CD3-positive T cells in any type of graft cells throughout the observation period (data not shown).

Apoptosis was considered as one reason of graft cell death [39], which was assessed in the graft cells using the TUNEL assay. Although the overall apoptosis rates in all cell types were low (Fig. 4C; PODs 1, 3, and 7, $n = 3$–4, PODs 14 and 21, $n = 5$–7), NSCs and MSCs demonstrated more TUNEL-positive cells at PODs 1 and 7 ($p < .05$) and POD 14 ($p < .05$), respectively, than iPS-RPE cells at each time point. Furthermore, the apoptotic cells in iPS-RPE graft cells remained consistently very low throughout the observation period.

Finally, we determined whether PEDF was elevated in iPS-RPE transplanted eyes because it is a major candidate among photoreceptor protective factors. In the collected IF, PEDF was significantly high during the first 3 weeks after transplantation, which corresponded to the time of significant photoreceptor protection (890 ± 615; 4,710 ± 1,495; and 2,453 ± 1,741 ng/ml at PODs 7, 14, and 21 [$n = 5$ for each time point], respectively). In contrast, PEDF levels in IF of MSCs and NSCs transplanted eyes, and sham eyes of iPS-RPE cell injected mice were nearly the same at any point tested (Fig. 4D; $p < .01$; $n = 5$ for iPS-RPE-grafted eyes, $n = 3$–5 for NSC, MSC, or sham eyes). Since the iPS-RPE cells transplanted fellow eyes had a higher number of remaining rod cells, we also compared PEDF concentration among all control eyes, which showed a higher average concentration of PEDF in iPS-RPE eyes compared with the other groups at POD 14, but with no statistical significance (Supporting Information Fig. S5; RPE vs. MSC, $p = .1$, RPE vs. NSC, $p = .8$).

Discussion

The results of our study suggest that RPE cells derived from human iPS cells are more effective than MSCs or NSCs in delaying photoreceptor cell loss after implantation into the subretinal space of a rapidly progressing retinal degeneration model, *rd1* mice. There were no graft-derived postoperative complications in any cell type group. In this model, the majority of rod photoreceptors degenerate within 3 weeks after birth. The transplantation was performed at week 2 after birth, corresponding to the timing when photoreceptor cell death is most drastic and dead cells are being rapidly swept away with maximum microglial accumulation [40]. This was concluded to be a harsh period for any type of transplanted cells to survive. Therefore, it is noteworthy that transplanted-iPS-RPE cells were more capable of surviving in this severe environment than the other cell types. These results are even more exciting considering that iPS-RPE cells were readily detectable as late as 3 months following transplantation. Considering the goal of cell therapy for the purpose of replacement therapy or trophic factor supplementation, the survival duration of graft cells is one of the most important factors.

In terms of iPS-RPE cell survival, all our data (e.g., mild proliferation, consistently low apoptosis rate, and minimal microglia accumulation in RPE grafts) support the fact that these cells are better suited to survive longer in the ocular environment. This may imply that these cells have a tolerance for survival in an adequate environment where they originally belong or that some intrinsic characteristics contribute to their survival. Although transplanted iPS-RPE cells showed a mild proliferation, there was no evidence of tumor-like formation up to at least 12 weeks after operation, and the graft cells nonetheless decreased gradually eventually forming a sheet-like structure with one or two layers (Fig. 3D, 3G; Supporting Information Fig. S2A, S2B). hiPS-RPE cells also survived for more than 5 months in an animal model of Leber congenital amaurosis, *rd12* (*RPE65*^{rd12}/*RPE65*^{rd12}) mice, supporting the stable viability of transplanted iPS-RPE cells [41]. However, Carr et al. [42] demonstrated that hiPS-RPE cells transplanted as xenografts were ultimately lost 13 weeks after surgery despite its long-term visual function maintenance in RCS rats where a different pathological environment may have affected graft survival: in RCS rats, RPE cells cannot phagocytose shed outer segments, and therefore transplanted RPE cells were shown to phagocytose accumulated segments that would have put these cells under stress, resulting in poorer graft survival. Transplanted human RPE cells were also reported to survive in the subretinal space of rabbits [43] and monkeys [44] for 3 and 6 months, respectively, even in the absence of immunosuppression. In contrast, transplantation of human NSCs into the subretinal space of nonimmunosuppressed pigs did not persist beyond the 4th week, mainly because of marked mononuclear cell reaction [45]. Another group injected immortalized human NSCs into the spinal cords of immunosuppressed rats and observed that the grafts were rejected after 4 weeks [39]. Several publications have shown that RPE cells display immunosuppressive properties by suppressing the activation of T lymphocytes via TGF-beta [46, 47] and by converting $CD4^+$ T cells into T regulatory (Treg) cells through TGF-beta signaling [48]. Moreover, in addition to its role in regulating T cells, TGF-beta functions to inhibit the activation and proliferation of microglia in a dose-dependent manner [37, 38, 49]. In fact, our ELISA assay demonstrated that iPS-RPE cells secreted a significant amount of TGF-beta 2. More interestingly, the accumulation of microglia was less drastic in iPS-RPE cells and NSCs than in MSCs, possibly because of their substantial secretion of TGF-beta 2 in comparison with MSCs. These data suggest that RPE cells have a unique immune competency in the ocular environment that enables their own survival following transplantation. The absence of $CD3^+$ T cells infiltration observed in all the cell-type grafts suggested that systemic T-cell-mediated immune rejection was basically suppressed by cyclosporine [50, 51] in our experiments but local immune or inflammatory reaction may have contributed to the rapid elimination of MSCs or NSCs.

In this study, we used *rd1* as a model of the most progressive retinal degeneration to test whether transplanted cells could intervene to delay photoreceptor loss, even during ongoing degeneration. Although the mechanisms of rapid photoreceptor cell death in *rd1* mice are extremely complicated, it may be primarily attributed to PDE6-beta mutation, followed by accompanying events such as an excess release of glutamate, downregulation in defensive mechanisms against oxidative stress, and unregulated immune reactions. In particular, PDE6-beta mutation leads to cGMP accumulation in rods that can lead to an increased influx of Na^+ and Ca^+ through cGMP-sensitive cation channels. This elevation in Ca^{2+} levels triggers apoptosis of photoreceptor cells in *rd1* mice [52]. Another study showed that uncontrolled glutamate release due to constant rod depolarization may compromise the synaptic connectivity between rod and bipolar cells, leading to "retrograde degeneration" of rods [53]. Downregulation of defensive mechanisms against oxidative stress in *rd1* mice may lead to an increase in intracellular reactive oxygen species that eventually induces endoplasmic reticulum stress and thereby triggers apoptosis of photoreceptor cells [54]. Microglia are referred to as a "double-edged sword" as they could be either protective or neurotoxic; they infiltrate around degenerating photoreceptor cells and may release proinflammatory cytokines to accelerate cell death [55].

Although it is difficult to clarify the detailed mechanisms by which transplanted RPE cells intervene with any of these processes, trophic factors secreted by RPE cells, particularly PEDF, may provide an explanation for their protective effect in this study. Neuroprotective effects of PEDF both on photoreceptors [9, 11, 56] and other types of neurons [7, 57, 58] have been reported, and iPS-RPE cells secreted more than 10- and 100-times higher concentration of PEDF than MSCs and NSCs in vitro, respectively (Fig. 1X). Transplanted iPS-RPE cells released a significantly high concentration of PEDF in vivo from shortly after transplantation (approximately 100-times and 4–500-times higher than NSCs and MSCs transplanted eyes at PODs 7 and 14, respectively) for more than 3 weeks (Fig. 4D). A single intravitreous injection of PEDF at a higher concentration was reported to demonstrate a transient delay (a couple of days) in photoreceptor loss in two different retinal degeneration models [11]. Considering a further dilution by IF and the short half-life of PEDF [59], transplanted iPS-RPE cells may act as a sustainable source of PEDF and provide a longer duration of neuroprotection. Unexpectedly, the fellow

eyes of iPS-RPE cells transplanted mice at POD 21 also showed a higher number of surviving rod cells compared to the fellow eyes of NSC transplantation, the cell type with least PEDF secretion in our experiments. Considering the continual high elevation of PEDF in the iPS-RPE cells transplanted eyes, it might have also affected the contralateral eye via systemic circulation. The average PEDF concentration at POD 14 in the fellow eyes in iPS-RPE transplanted groups was highest among all the groups even though the increase was not statistically significant (Supporting Information Fig. S5). The photoreceptors, located in most proximity to choroid circulation, could have been exposed to higher concentrations of PEDF at some time point in iPS-RPE transplanted group. The effect on the fellow eyes of intraocular injections of anti-VEGF compounds, ranibizumab and bevacizumab, has been reported in clinical cases, suggesting that a high concentration in one eye could in fact affect the other eye [60–62]. Bevacizumab was also detected in the contralateral eyes in rabbits [63] after intraocular injection, and considering the molecular weight of ranibizumab (48.39 kDa) and bevacizumab (149 kDa) [64], PEDF (50 kDa) [65] may similarly distribute to the fellow eyes. Moreover, several studies have reported that VEGF, beta-NGF, and NT-3 exhibited rescue effects on various neurons, including photoreceptors [66–73]. Thus, in this study, these factors secreted by iPS-RPE cells may also have additionally contributed to attenuating photoreceptor death in *rd1* mice.

Three important aspects of using human iPS-RPE cells are as follows: (a) iPS-derived cells do not raise ethical concerns, (b) iPS-RPE cells survive well in the subretinal space because of their immune suppressive potency and possibly their native residence, and (c) because iPS-RPE cells secrete multiple neurotrophic factors, including PEDF, they can help preserve photoreceptor cells in various pathological situations without additional manipulation. Previous studies used genetically modified NSCs that expressed neurotrophic factors for the prevention of neuron death [74–76], among which CNTF gene-modified NSCs could rescue photoreceptor loss in *rd1* mice, while nonmodified NSCs could not [76].

RPE transplantation may be reasonably considered effective in RP patients with RPE-associated gene mutations such as RPE65, MERTK, and LRAT [3, 4, 77]. Li et al. and Maeda et al. independently showed that graft survival and functional rescue were observed after the transplantation of iPS-RPE cells into the subretinal space of *rd12* and *Lrat*$-/-$ mice. In these models, the host RPE cells cannot convert all-trans retinal to 11-cis retinal and cannot supply visual pigments to photoreceptors and iPS-RPE cells restored that function [41, 77]. Additionally, in many inherited and acquired retinal degenerative disorders, there is usually a sequential degeneration of both RPE cells and photoreceptors, and this study indicates that RPE as a source of PEDF and other trophic factors would also be valuable for a larger clinical application than specific functional restoration. The clinical course of RP is very long and often accompanies RPE atrophy [78, 79], and, as such, human iPS-RPE cell transplantation may be an option for delaying photoreceptor cell loss in RP patients with any causal genes. Because the ocular space in humans is much larger than that in mice, it may be necessary to provide 1,000 times the number of cells used in this study to achieve the corresponding intraocular concentrations of neurotrophic factors in human eyes. However, transplanted RPE cells should still have a local effect on overlying photoreceptors, even with a lower number than that described above. The protective potency in relation to the number of transplanted RPE cells must be further validated. Furthermore, a possibility for another application of iPS-RPE transplantation is the dry-type and also the wet-type AMD, which accompanies choroidal neovascularization. It has been shown that PEDF may oppose the angiogenic potential of VEGF [80–82], a key factor leading to wet AMD, and RPE atrophy often persists even with current therapy such as anti-VEGF injections [83]. Thus, considering its strong survival potency, protective effect, and anti-inflammatory nature, iPS-RPE cell transplantation may also be promising for the protection of photoreceptors in inflammatory, progressive diseases, including wet-type AMD.

Conclusions

In comparison with MSCs and NSCs, subretinal transplanted iPS-RPE cells displayed significant rescue effects in protecting photoreceptors from degeneration in *rd1* mice, which may have been attributed to the continuous secretion of a high amount of PEDF. Human iPS-RPE cells survived longer than MSCs or NSCs, possibly because of consistently low apoptosis rate, and minimal microglia accumulation in RPE grafts. Thus, iPS-RPE cells may provide promising therapeutic benefits for patients suffering from retinal degenerative diseases, such as RP or AMD.

Acknowledgments

We thank Tadao Maeda, Kyoko Iseki, Noriko Sakai, and Satoshi Okamoto for technical assistance and advice and all members of the Takahashi Laboratory for valuable discussion and comments. J.S. also thanks the Japanese Government (Monbukagakusho: MEXT) Scholarship Program. This study was supported by a grant from the Project for Realization of Regenerative Medicine, MEXT.

Author Contributions

J.S.: conception and design, collection and/or assembly of data, data analysis and interpretation, manuscript writing, and final approval of manuscript; M.M.: conception and design, data analysis and interpretation, manuscript writing, and final approval of manuscript; H.K.: collection and/or assembly of data; T.H.: technical support and data analysis and interpretation; M.S. and S.K.: provision of study material; S.S.: data analysis and interpretation and provision of study material; M.T.: conception and design, data analysis and interpretation, financial support, and final approval of manuscript.

Disclosure of Potential Conflicts of Interest

The authors indicate no potential conflicts of interest.

References

1 Strauss O. The retinal pigment epithelium in visual function. Physiol Rev 2005;85:845–881.

2 Li LX, Turner JE. Inherited retinal dystrophy in the RCS rat: Prevention of photoreceptor degeneration by pigment epithelial cell transplantation. Exp Eye Res 1988;47:911–917.

3 Bowne SJ, Humphries MM, Sullivan LS et al. A dominant mutation in RPE65 identified by whole-exome sequencing causes retinitis pigmentosa with choroidal involvement. Eur J Hum Genet 2011;19:1074–1081.

4 Gal A, Li Y, Thompson DA et al. Mutations in MERTK, the human orthologue of the RCS rat retinal dystrophy gene, cause retinitis pigmentosa. Nat Genet 2000;26:270–271.

5 Tombran-Tink J, Chader GG, Johnson LV. PEDF: A pigment epithelium-derived factor with potent neuronal differentiative activity. Exp Eye Res 1991;53:411–414.

6 Kanemura H, Go MJ, Nishishita N et al. Pigment epithelium-derived factor secreted from retinal pigment epithelium facilitates apoptotic cell death of iPSC. Sci Rep 2013;3:2334.

7 Taniwaki T, Hirashima N, Becerra SP et al. Pigment epithelium-derived factor protects cultured cerebellar granule cells against glutamate-induced neurotoxicity. J Neurochem 1997;68:26–32.

8 Cao W, Tombran-Tink J, Chen W et al. Pigment epithelium-derived factor protects cultured retinal neurons against hydrogen peroxide-induced cell death. J Neurosci Res 1999;57:789–800.

9 Cao W, Tombran-Tink J, Elias R et al. In vivo protection of photoreceptors from light damage by pigment epithelium-derived factor. Invest Ophthalmol Vis Sci 2001;42:1646–1652.

10 Takita H, Yoneya S, Gehlbach PL et al. Retinal neuroprotection against ischemic injury mediated by intraocular gene transfer of pigment epithelium-derived factor. Invest Ophthalmol Vis Sci 2003;44:4497–4504.

11 Cayouette M, Smith SB, Becerra SP et al. Pigment epithelium-derived factor delays the death of photoreceptors in mouse models of inherited retinal degenerations. Neurobiol Dis 1999;6:523–532.

12 Fischer AJ, Bongini R. Turning Müller glia into neural progenitors in the retina. Mol Neurobiol 2010;42:199–209.

13 Coles BL, Angenieux B, Inoue T et al. Facile isolation and the characterization of human retinal stem cells. Proc Natl Acad Sci USA 2004;101:15772–15777.

14 Kicic A, Shen WY, Wilson AS et al. Differentiation of marrow stromal cells into photoreceptors in the rat eye. J Neurosci 2003;23:7742–7749.

15 Arnhold S, Absenger Y, Klein H et al. Transplantation of bone marrow-derived mesenchymal stem cells rescue photoreceptor cells in the dystrophic retina of the rhodopsin knockout mouse. Graefes Arch Clin Exp Ophthalmol 2007;245:414–422.

16 Xiong N, Zhang Z, Huang J et al. VEGF-expressing human umbilical cord mesenchymal stem cells, an improved therapy strategy for Parkinson's disease. Gene Ther 2011;18:394–402.

17 Pressmar S, Ader M, Richard G et al. The fate of heterotopically grafted neural precursor cells in the normal and dystrophic adult mouse retina. Invest Ophthalmol Vis Sci 2001;42:3311–3319.

18 McGill TJ, Cottam B, Lu B et al. Transplantation of human central nervous system stem cells—Neuroprotection in retinal degeneration. Eur J Neurosci 2012;35:468–477.

19 Pluchino S, Quattrini A, Brambilla E et al. Injection of adult neurospheres induces recovery in a chronic model of multiple sclerosis. Nature 2003;422:688–694.

20 Barhoum R, Martinez-Navarrete G, Corrochano S et al. Functional and structural modifications during retinal degeneration in the rd10 mouse. Neuroscience 2008;155:698–713.

21 Bowes C, Li T, Danciger M et al. Retinal degeneration in the rd mouse is caused by a defect in the beta subunit of rod cGMP-phosphodiesterase. Nature 1990;347:677–680.

22 Kamao H, Mandai M, Okamoto S et al. Characterization of human induced pluripotent stem cell-derived retinal pigment epithelium cell sheets aiming for clinical application. Stem Cell Reports 2014;2:205–218.

23 Dominici M, Le Blanc K, Mueller I et al. Minimal criteria for defining multipotent mesenchymal stromal cells. The International Society for Cellular Therapy position statement. Cytotherapy 2006;8:315–317.

24 Halfon S, Abramov N, Grinblat B et al. Markers distinguishing mesenchymal stem cells from fibroblasts are downregulated with passaging. Stem Cells Dev 2011;20:53–66.

25 Covas DT, Panepucci RA, Fontes AM et al. Multipotent mesenchymal stromal cells obtained from diverse human tissues share functional properties and gene-expression profile with CD146+ perivascular cells and fibroblasts. Exp Hematol 2008;36:642–654.

26 Lund RD, Wang S, Lu B et al. Cells isolated from umbilical cord tissue rescue photoreceptors and visual functions in a rodent model of retinal disease. Stem Cells 2007;25:602–611.

27 Wagner W, Horn P, Castoldi M et al. Replicative senescence of mesenchymal stem cells: A continuous and organized process. PLoS One 2008;3:e2213.

28 Gamm DM, Melvan JN, Shearer RL et al. A novel serum-free method for culturing human prenatal retinal pigment epithelial cells. Invest Ophthalmol Vis Sci 2008;49:788–799.

29 Gamm DM, Wang S, Lu B et al. Protection of visual functions by human neural progenitors in a rat model of retinal disease. PLoS One 2007;2:e338.

30 Tombran-Tink J, Shivaram SM, Chader GJ et al. Expression, secretion, and age-related downregulation of pigment epithelium-derived factor, a serpin with neurotrophic activity. J Neurosci 1995;15:4992–5003.

31 Ishida K, Yoshimura N, Yoshida M et al. Expression of neurotrophic factors in cultured human retinal pigment epithelial cells. Curr Eye Res 1997;16:96–101.

32 Martino G, Pluchino S. The therapeutic potential of neural stem cells. Nat Rev Neurosci 2006;7:395–406.

33 Klassen HJ, Imfeld KL, Kirov II et al. Expression of cytokines by multipotent neural progenitor cells. Cytokine 2003;22:101–106.

34 Zhang Y, Wang W. Effects of bone marrow mesenchymal stem cell transplantation on light-damaged retina. Invest Ophthalmol Vis Sci 2010;51:3742–3748.

35 Wang J, Liao L, Tan J. Mesenchymal-stem-cell-based experimental and clinical trials: Current status and open questions. Expert Opin Biol Ther 2011;11:893–909.

36 Horwitz EM, Dominici M. How do mesenchymal stromal cells exert their therapeutic benefit? Cytotherapy 2008;10:771–774.

37 Suzumura A, Sawada M, Yamamoto H et al. Transforming growth factor-beta suppresses activation and proliferation of microglia in vitro. J Immunol 1993;151:2150–2158.

38 Jones LL, Kreutzberg GW, Raivich G. Transforming growth factor beta's 1, 2 and 3 inhibit proliferation of ramified microglia on an astrocyte monolayer. Brain Res 1998;795:301–306.

39 Li P, Tessler A, Han SS et al. Fate of immortalized human neuronal progenitor cells transplanted in rat spinal cord. Arch Neurol 2005;62:223–229.

40 Mandai M, Homma K, Okamoto S et al. Adequate time window and environmental factors supporting retinal graft cell survival in rd mice. Cell Med 2012;4:45–54.

41 Li Y, Tsai YT, Hsu CW et al. Long-term safety and efficacy of human-induced pluripotent stem cell (iPS) grafts in a preclinical model of retinitis pigmentosa. Mol Med 2012;18:1312–1319.

42 Carr AJ, Vugler AA, Hikita ST et al. Protective effects of human iPS-derived retinal pigment epithelium cell transplantation in the retinal dystrophic rat. PLoS One 2009;4:e8152.

43 He S, Wang HM, Ogden TE et al. Transplantation of cultured human retinal pigment epithelium into rabbit subretina. Graefes Arch Clin Exp Ophthalmol 1993;231:737–742.

44 Berglin L, Gouras P, Sheng Y et al. Tolerance of human fetal retinal pigment epithelium xenografts in monkey retina. Graefes Arch Clin Exp Ophthalmol 1997;235:103–110.

45 Warfvinge K, Schwartz PH, Kiilgaard JF et al. Xenotransplantation of human neural progenitor cells to the subretinal space of nonimmunosuppressed pigs. J Transplant 2011;2011:948740.

46 Sugita S, Futagami Y, Smith SB et al. Retinal and ciliary body pigment epithelium suppress activation of T lymphocytes via transforming growth factor beta. Exp Eye Res 2006;83:1459–1471.

47 Vega JL, Saban D, Carrier Y et al. Retinal pigment epithelial cells induce foxp3(+) regulatory T cells via membrane-bound TGF-beta. Ocul Immunol Inflamm 2010;18:459–469.

48 Sugita S, Horie S, Nakamura O et al. Retinal pigment epithelium-derived CTLA-2alpha induces TGFbeta-producing T regulatory cells. J Immunol 2008;181:7525–7536.

49 Paglinawan R, Malipiero U, Schlapbach R et al. TGFbeta directs gene expression of activated microglia to an anti-inflammatory phe-

notype strongly focusing on chemokine genes and cell migratory genes. Glia 2003;44:219–231.
50 Matsuda S, Koyasu S. Mechanisms of action of cyclosporine. Immunopharmacology 2000;47:119–125.
51 Shii D, Nakagawa S, Shinomiya K et al. Cyclosporin A eye drops inhibit fibrosis and inflammatory cell infiltration in murine type I allergic conjunctivitis without affecting the early-phase reaction. Curr Eye Res 2009;34: 426–437.
52 Frasson M, Sahel JA, Fabre M et al. Retinitis pigmentosa: Rod photoreceptor rescue by a calcium-channel blocker in the rd mouse. Nat Med 1999;5:1183–1187.
53 Delyfer MN, Forster V, Neveux N et al. Evidence for glutamate-mediated excitotoxic mechanisms during photoreceptor degeneration in the rd1 mouse retina. Mol Vis 2005; 11:688–696.
54 Ahuja-Jensen P, Johnsen-Soriano S, Ahuja S et al. Low glutathione peroxidase in rd1 mouse retina increases oxidative stress and proteases. Neuroreport 2007;18:797–801.
55 Wright AF, Chakarova CF, Abd El-Aziz MM et al. Photoreceptor degeneration: Genetic and mechanistic dissection of a complex trait. Nat Rev Genet 2010;11:273–284.
56 Murakami Y, Ikeda Y, Yonemitsu Y et al. Inhibition of nuclear translocation of apoptosis-inducing factor is an essential mechanism of the neuroprotective activity of pigment epithelium-derived factor in a rat model of retinal degeneration. Am J Pathol 2008;173:1326–1338.
57 Bilak MM, Corse AM, Bilak SR et al. Pigment epithelium-derived factor (PEDF) protects motor neurons from chronic glutamate-mediated neurodegeneration. J Neuropathol Exp Neurol 1999;58:719–728.
58 Houenou LJ, D'Costa AP, Li L et al. Pigment epithelium-derived factor promotes the survival and differentiation of developing spinal motor neurons. J Comp Neurol 1999; 412:506–514.
59 Bai YJ, Huang LZ, Xu XL et al. Polyethylene glycol-modified pigment epithelial-derived factor: New prospects for treatment of retinal neovascularization. J Pharmacol Exp Ther 2012;342:131–139.
60 Acharya NR, Sittivarakul W, Qian Y et al. Bilateral effect of unilateral ranibizumab in patients with uveitis-related macular edema. Retina 2011;31:1871–1876.
61 Hanhart J, Tiosano L, Averbukh E et al. Fellow eye effect of unilateral intravitreal bevacizumab injection in eyes with diabetic macular edema. Eye (Lond) 2014;28: 646–653.
62 Wu Z, Sadda SR. Effects on the contralateral eye after intravitreal bevacizumab and ranibizumab injections: A case report. Ann Acad Med Singapore 2008;37: 591–593.
63 Nomoto H, Shiraga F, Kuno N et al. Pharmacokinetics of bevacizumab after topical, subconjunctival, and intravitreal administration in rabbits. Invest Ophthalmol Vis Sci 2009;50:4807–4813.
64 Zou L, Lai H, Zhou Q et al. Lasting controversy on ranibizumab and bevacizumab. Theranostics 2011;1:395–402.
65 Tombran-Tink J, Barnstable CJ. PEDF: A multifaceted neurotrophic factor. Nat Rev Neurosci 2003;4:628–636.
66 Azzouz M, Ralph GS, Storkebaum E et al. VEGF delivery with retrogradely transported lentivector prolongs survival in a mouse ALS model. Nature 2004;429:413–417.
67 Sun Y, Jin K, Xie L et al. VEGF-induced neuroprotection, neurogenesis, and angiogenesis after focal cerebral ischemia. J Clin Invest 2003;111:1843–1851.
68 Tovar YRLB, Tapia R. VEGF protects spinal motor neurons against chronic excitotoxic degeneration in vivo by activation of PI3-K pathway and inhibition of p38MAPK. J Neurochem 2010;115:1090–1101.
69 Semkova I, Haberlein C, Krieglstein J. Ciliary neurotrophic factor protects hippocampal neurons from excitotoxic damage. Neurochem Int 1999;35:1–10.
70 Zhu L, Du F, Yang L et al. Nerve growth factor protects the cortical neurons from chemical hypoxia-induced injury. Neurochem Res 2008;33:784–789.
71 Lambiase A, Aloe L. Nerve growth factor delays retinal degeneration in C3H mice. Graefes Arch Clin Exp Ophthalmol 1996; 234(suppl 1):S96–S100.
72 Carnicero E, Knipper M, Tan J et al. Herpes simplex virus type 1-mediated transfer of neurotrophin-3 stimulates survival of chicken auditory sensory neurons. Neurosci Lett 2002;321:149–152.
73 Shen W, Zhu L, Lee SR et al. Involvement of NT3 and P75(NTR) in photoreceptor degeneration following selective Muller cell ablation. J Neuroinflammation 2013;10:137.
74 Akerud P, Canals JM, Snyder EY et al. Neuroprotection through delivery of glial cell line-derived neurotrophic factor by neural stem cells in a mouse model of Parkinson's disease. J Neurosci 2001;21:8108–8118.
75 Martinez-Serrano A, Lundberg C, Horellou P et al. CNS-derived neural progenitor cells for gene transfer of nerve growth factor to the adult rat brain: Complete rescue of axotomized cholinergic neurons after transplantation into the septum. J Neurosci 1995;15:5668–5680.
76 Jung G, Sun J, Petrowitz B et al. Genetically modified neural stem cells for a local and sustained delivery of neuroprotective factors to the dystrophic mouse retina. Stem Cells Transl Med 2013;2:1001–1010.
77 Maeda T, Lee MJ, Palczewska G et al. Retinal pigmented epithelial cells obtained from human induced pluripotent stem cells possess functional visual cycle enzymes in vitro and in vivo. J Biol Chem 2013;288: 34484–34493.
78 Hashimoto Y, Kase S, Saito W et al. Abnormalities of fundus autofluorescence in pigmented paravenous chorioretinal atrophy. Open Ophthalmol J 2012;6:125–128.
79 Mitamura Y, Mitamura-Aizawa S, Nagasawa T et al. Diagnostic imaging in patients with retinitis pigmentosa. J Med Invest 2012;59:1–11.
80 Bhutto IA, McLeod DS, Hasegawa T et al. Pigment epithelium-derived factor (PEDF) and vascular endothelial growth factor (VEGF) in aged human choroid and eyes with age-related macular degeneration. Exp Eye Res 2006;82:99–110.
81 Amaral J, Becerra SP. Effects of human recombinant PEDF protein and PEDF-derived peptide 34-mer on choroidal neovascularization. Invest Ophthalmol Vis Sci 2010;51:1318–1326.
82 Mori K, Duh E, Gehlbach P et al. Pigment epithelium-derived factor inhibits retinal and choroidal neovascularization. J Cell Physiol 2001;188:253–263.
83 Rosenfeld PJ, Shapiro H, Tuomi L et al. Characteristics of patients losing vision after 2 years of monthly dosing in the phase III ranibizumab clinical trials. Ophthalmology 2011;118:523–530.

See www.StemCells.com for supporting information available online.

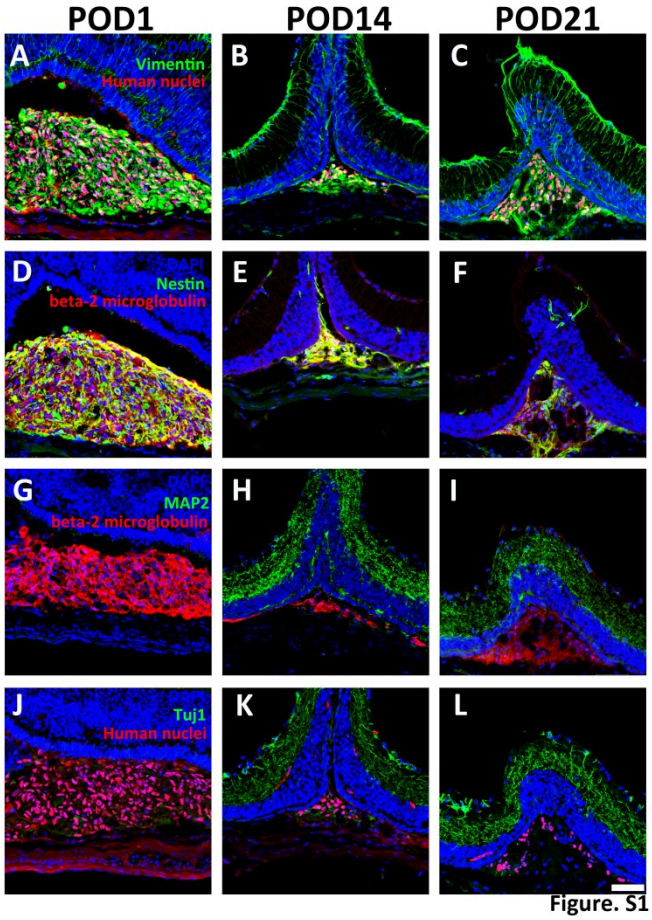
POD1
POD14
POD21
A
Vimentin
Human nuclei
B
C
D
Nestin
beta-2 microglobulin
E
F
G
MAP2
beta-2 microglobulin
H
I
J
Tuj1
Human nuclei
K
L

Figure. S1

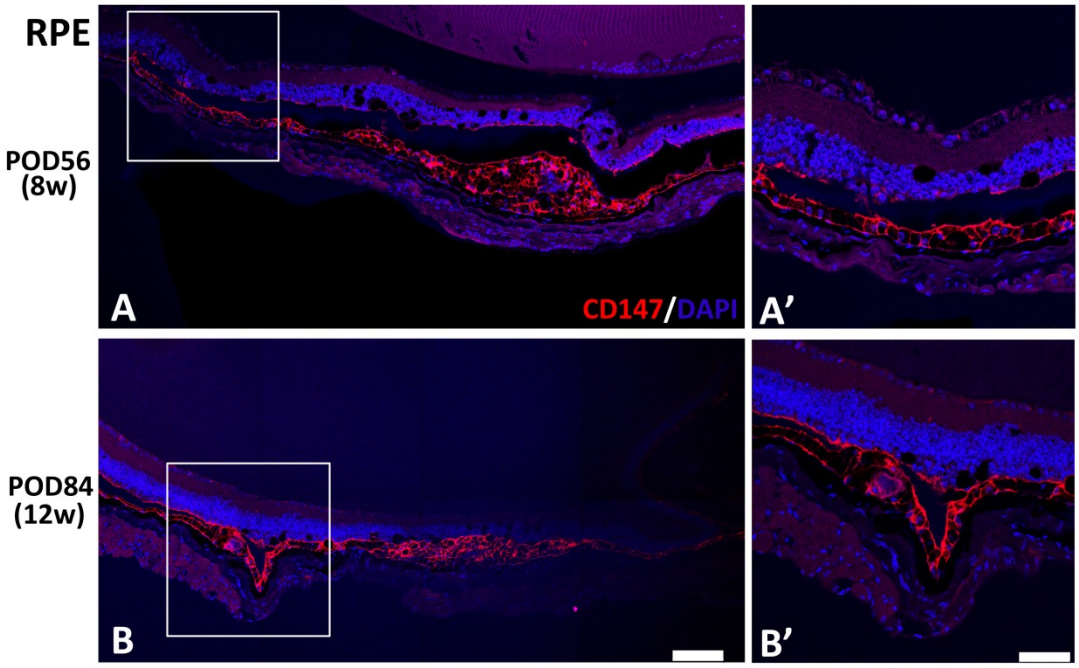

Figure. S2

Figure. S3

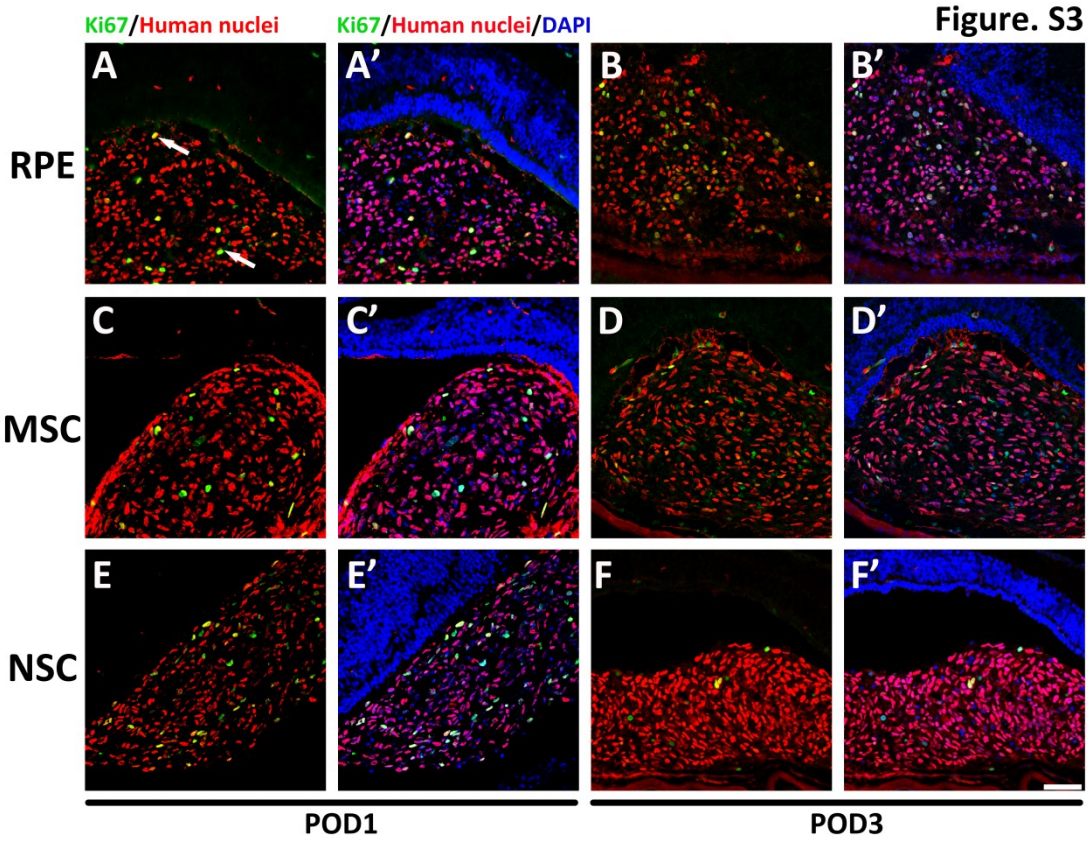

Figure.S4

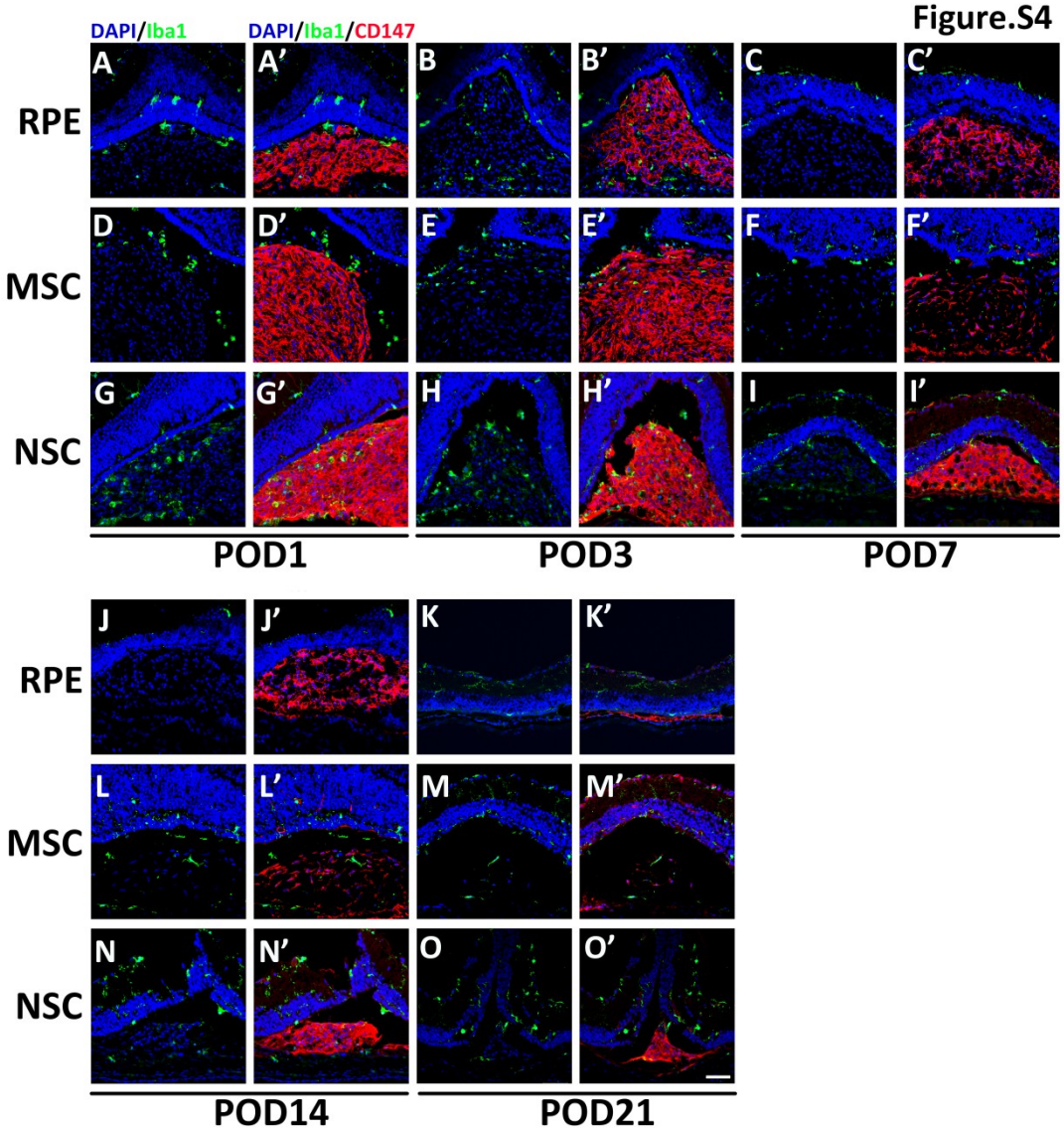

Figure.S5

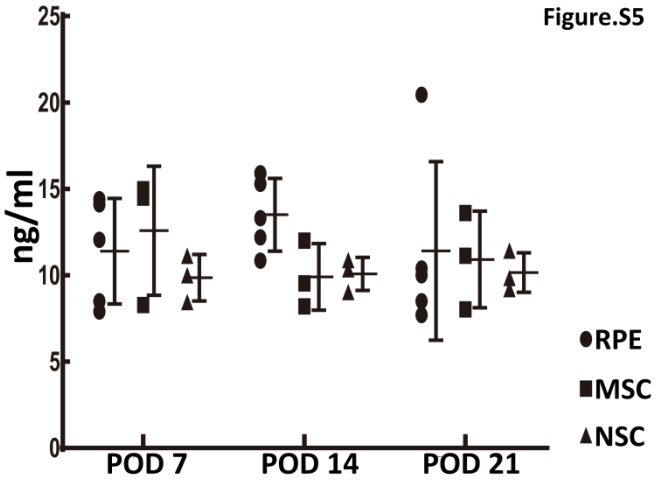

Supporting experimental procedures

Culture of hiPS-RPE cells

iPS-derived RPE cells were cultured on CELLstart-coated dishes (Life Technologies, Carlsbad, CA, USA) in maintenance medium [1] consisting of DMEM, F-12 Ham, 2 mM L-glutamine (all from Sigma-Aldrich, St. Louis, MO, USA), B27, penicillin–streptomycin (both from Life Technologies), 10 ng/ml recombinant human basic fibroblast growth factor (bFGF) (Wako, Osaka, Japan), and 0.5 μM SB431542 (Sigma-Aldrich).

Culture of NSCs

NSCs were cultured on laminin-coated dishes in RHB-A medium (StemCells) supplemented with 20 ng/ml of both recombinant human epidermal growth factor (EGF) (PeproTech, Rocky Hill, NJ, USA) and recombinant human bFGF (Wako).

Culture of MSCs

Human MSCs were established from the connective tissue of the umbilical cord vein. A scalpel was used to cut the connective tissues into small blocks (2 × 2 × 2 mm), and approximately 50 tissue-blocks were placed into a 10-cm dish. Cells were cultured for 7 days with 10 ml of Alpha-MEM (Life Technologies) supplemented with 10% FCS (Sigma-Aldrich) and penicillin–streptomycin (Life Technologies). Adherent cells spread on the dish with a uniform morphology were harvested with 0.05% Trypsin–EDTA (Life Technologies) and maintained with commercially available MSC culture medium (Toyobo, Osaka, Japan).

All three cell types were cultured under standard atmospheric conditions and 5% carbon dioxide at 37°C. For each cell type, the medium was changed every other day, and each cell type was characterized before use.

Flow cytometry

MSCs were washed with PBS (Life Technologies), trypsinized, and resuspended in buffer [1% FBS in PBS] at a concentration of 2×10^3 cells/μl. Cells were incubated with each antibody following the manufacturer's protocols, with isotype IgGs serving as controls. Following incubation, the cells were rinsed with 1% FBS buffer and resuspended in 500 μl of the same buffer. Analysis was performed using the FACSCanto II (BD Biosciences), and data were compiled with FlowJo software (Treestar, Ashland, OR, USA).

Immunostaining

iPS-RPE cells and NSCs cultured on eight-well chamber slides (BD Biosciences) were fixed in 4% paraformaldehyde (PFA) for 15 min at 4°C. After two PBS washes, samples were exposed to 0.3% Triton X-100 in PBS (w/v) for 30 min to permeabilize cellular membranes. Cells were then blocked with 5% donkey serum in PBS for 1 h at room temperature (RT). Primary antibodies were diluted in antibody diluent (Dako, Glostrup, Denmark) and incubated with the blocked samples overnight to detect nestin, beta-3 tubulin (Tuj1), MAP2, vimentin, bestrophin, RPE65, MITF, and ZO-1 (Supporting information, Table1). Samples were then rinsed three times with 0.05% Tween-20 in PBS (w/v), following which sections were incubated with the appropriate secondary antibodies for 1 h at room temperature and counterstained with DAPI (Life Technologies). Images were acquired using a confocal microscope (Zeiss, Oberkochen, Germany).

After mice were sacrificed by cervical dislocation, the eyes were enucleated and fixed in 4% PFA at room temperature for 30 min. The eyes were then washed with PBS, followed by the removal of the cornea, iris, and lens under a microscope (Olympus, Tokyo, Japan).

For cryosection preparation, the eyes were infiltrated with 30% sucrose overnight at 4°C and embedded in optimum cutting temperature (O.C.T) compound (Sakura, Alphen aan den Rijn, Netherlands). Ten-μm-thick sections were cut in a coronal plane on a cryostat (Thermo, Waltham, MA, USA) in sequential five slide series. The eyes collected at the 8th and 12th weeks were fixed and embedded in paraffin (Sigma-Aldrich); at this point, sections were

sliced using an auto slide preparation system (Kurabo, Osaka, Japan) in the same pattern as that used for cryosectioning. Although the retina was confirmed to be attached at the time of harvest, the abovementioned procedure may have caused preparatory retinal detachment (artifact) in some samples. Additional primary antibodies against the following proteins were used: human Ki67, human CD147, human nuclei antigen, human beta-2 microglobulin, Iba1, CD3, and rhodopsin (Supporting information, Table1). For these experiments, we applied the same immunochemical techniques and photographing methods as those mentioned above.

1 Gamm DM, Melvan JN, Shearer RL et al. A novel serum-free method for culturing human prenatal retinal pigment epithelial cells. Invest Ophthalmol Vis Sci 2008;49:788–799.

Supporting information Table 1

Antibody	**Type**	**Source**	**Dilution**
Nestin	Mouse	Covance (MMS-570P)	1:8000
Tuj1	Rabbit	Covance (MRB-435P)	1:32000
Map2	Mouse	Sigma-Aldrich (M4403)	1:8000
Vimentin	Rabbit	Biovison (3634-100)	1:800
Bestrophin	Mouse	Abcam (AB2182)	1:500
RPE65	Rabbit	Developed in our laboratory[1]	1:1000
Mitf	Mouse	Abcam (AB2384)	1:500
Zo-1	Rabbit	Life technologies (61-7300)	1:100
Retp1	Mouse	Sigma-Aldrich (O4886)	1:10000
Human nuclei	Mouse	Millipore (MAB1281)	1:2000
CD147	Goat	R&D system (AF972)	1:200
beta-2 microglobulin	Rabbit	Abcam (Ab15976)	1:1000
Ki67	Rabbit	Epitomics (4203-1)	1:1000
Iba1	Rabbit	Wako (019-19741)	1: 4000
CD3	Goat	Santa Cruz Biotechnology (SC-1127)	1:1000

1 Osakada F, Ikeda H, Mandai M et al. Toward the generation of rod and cone photoreceptors from mouse, monkey and human embryonic stem cells. Nat Biotechnol 2008;26:215–224.

Supporting Information Figure S1: Undifferentiated state of grafted NSCs was maintained until POD 21. (A–L) NSCs expressed immature markers, vimentin (A–C) (note that vimentin also labeled host Müller cells) and nestin (D–F), but did not express mature markers, MAP2 (G–I) and Tuj1 (J–L) (host ganglion cells were positive for MAP2 and Tuj1). All human cells were identified with human nuclear or human beta-2 microglobulin markers. Scale bar in L = 50 μm (also applies to A–K).

Supporting Information Figure S2: Subretinal grafted iPS-RPE cells survived up to 8 (POD 56) and 12 (POD 84) weeks postoperatively. (A, B) A portion of iPS-RPE grafts formed a sheet-like structure in the subretinal space. (A', B') High magnification of the boxed region in panel B and C, respectively. Scale bar in B = 100 μm (also applies to A); scale bar in B' = 50 μm (also applies to A').

Supporting Information Figure S3: Proliferating cells in the grafts at PODs 1 and 3 (related to Figure 4A). (A–F) Representative immunostaining images display grafts stained with proliferation marker Ki67 (arrow) as well as a human nuclear marker. More Ki67-positive cells were observed in NSC grafts at POD 1 (E) and in iPS-RPE grafts at POD 3 (B). Scale bar in F' = 50 μm (also applies to the rest).

Supporting Information Figure S4: Immunohistochemistry images of microglial infiltration at different time points (related to Figure 4B). (A–O) Images with DAPI and Iba1 staining are shown. (A'–O') Images corresponding to panels A to O with additional CD147 staining are shown. Scale bar in O' = 50 μm (also applies to the rest).

Supporting Information Figure S5: The concentrations of PEDF in the IF of the fellow eyes following the subretinal transplantation of iPS-RPE cells, MSCs, and NSCs at PODs 7, 14, and 21. The mean concentration of PEDF in the contralateral eye of iPS-RPE cells transplanted eyes were higher compared with other groups at POD 14, although there was no statistical significance (RPE vs. MSC, $p = 0.1$, RPE vs. NSC, $p = 0.8$).